Novel Anionic Polymerization of ε-Caprolactam Towards Polyamide 6 Containing Nanofibrils

Shervin Ahmadi[1*], Jalil Morshedian[1], Seyed Ali Hashemi[1],
Pierre J Carreau[2], and Weawkamol Leelapornpisit[2]

(1) Iran Polymer and Petrochemical Institute, P.O. Box: 14965/115, Tehran, Iran
(2) Center for Applied Research on Polymers and Composites (CREPEC), Chemical
Engineering Department, École Polytechnique, Montréal, QC H3C 3A7, Canada

A B S T R A C T

Anionic ring-opening polymerization of ε-caprolactam leads to the formation of polyamide 6 (PA6). This reaction takes place at a significantly faster reaction rate and gives a narrower molecular weight distribution than the other techniques. Due to this advantage, anionic polymerization of ε-caprolactam towards PA6 in melt blending was investigated in this work. PA6 was prepared in an internal mixer via melt polymerization of ε-caprolactam as a monomer with sodium caprolactam as its catalyst and hexamethylene diisocyanate as an activator. The effects of various concentrations of catalyst and activator on the initiation time of the reaction and on the residual monomer were determined. The residual monomer was collected using a solvent extraction method and determined by GC-mass technique. The physical and mechanical properties of the PA6 prepared via melt blending and of a commercial PA6 prepared were determined by differential scanning calorimetry (DSC), thermal gravimetric analysis (TGA), tensile and impact tests. The experimental results showed that addition of 3% catalyst and 3% activator to the formulation gave the best properties. These conditions led to the lowest residual monomer and better mechanical properties as well. The other novel aspect of this investigation was the formation of nanofibril during melt polymerization of ε-caprolactam. Mechanical properties showed that the PA6 prepared by using this technique and the above formulation were similar to the PA6 commercial grade.

INTRODUCTION

Activated anionic polymerization of ε-caprolactam occurs at a significantly faster rate than the other techniques, e.g., hydrolytic systems. Anionic polymerization of ε-caprolactam has been used for the direct fabrication of parts via monomer casting or reaction injection moulding (RIM). High residual monomer and low mechanical properties are characteristics of the products in comparison with hydrolytic polymerized PA6 parts [1-4]. The presence of an anionically activated monomer and an activator are the essential conditions for starting the anionic polymerization of ε-caprolactam, which is most often found as an alkaline salt. The anionic polymerization of ε-caprolactam requires the presence of an anionically activated monomer, the lactam anion [1]. By the reaction of ε-caprolactam with the ε-caprolactam anion, an *N*-acyllactam

(∗) To whom correspondence to be addressed.
E-mail: sh.ahmadi@ippi.ac.ir

structure (a non-ionic growth centre of polymerization) is formed. Propagation consists in a repeated addition of the lactam anion on the carbonyl of the preformed *N*-acyllactam group [2]. The polymerization can be accelerated by addition of substances having *N*-acyllactam structure (direct activators) or by forming *N*-acyllactam structure in situ through the reaction of lactam with anhydrides, chlorides, esters, isocyanates, etc. (indirect activators) [2,3]. These substances are considered to be the activators of anionic polymerization.

The catalyst and activator are key components of the anionic ε-caprolactam polymerization and consequently its reaction kinetics. The degree of polymerization and other properties of the resulting polymer depend on the type, method of preparation, quality and quantity of the activator and catalyst. Only the correct ratios of monomer, activator and catalyst would ensure a complete reaction, which means it would give the least monomer residue [1,3]. Moreover, the processing parameters and techniques may also affect the degree of polymerization, which is the critical parameter for PA6 properties [1,5,6]. In their work, Fornes et al. [7] have established the existence of two crystalline forms of PA6, i.e., an α-phase and a thermodynamically less stable γ-phase, giving rise to the wide angle X-ray diffraction (WAXD) peaks at 19.6° (α_1), 23.5° (α_2) and 21.3° (γ). Anionic polymerized PA6, which was prepared in this study, showed three absorptions in agreement with the results obtained by Fornes et al. Also, in this work, by using sodium caprolactam together with an activator, i.e., hexamethylene diisocyanate (HDI) and specific process conditions, e.g., temperature, mixing conditions etc., we reduced the residual monomer content compared to the other techniques. In situ fibrillation of low viscosity dispersed phase in a high viscosity matrix during a shear media is a known fact which has been reported in many articles. For example micro- or nanofibril composites (MFCs or NFCs) are created by blending two polymers which have different melt viscosities such as PE and PET [8,9]. We finally investigated the morphology of the anionic polymerized PA6. In this research our objective was to study fibril morphology in a simultaneous process which had not been observed in other research works.

EXPERIMENTAL

Materials
The monomer used in this project was ε-caprolactam supplied by BASF Co., Germany. Hexamethylene diisocyanate (HDI), used as an activator, was obtained from Rhodia, France. The catalyst, sodium caprolactam was prepared via the reaction of sodium and caprolactam in a glass reactor under nitrogen atmosphere at 120°C for 35 min. For comparison, the mechanical properties of PA6 commercial grade, Akulon®F236 from DSM, Netherlands, were used as reference.

PA6 Preparation
Polymerization of ε-caprolactam (Table 1) was carried out in a 300 mL chamber of a Haake type internal mixer model Sys 9000 for sample preparation and subsequent evaluations. The rotor speed during compounding was fixed at 150 rpm. The mixing time for all samples was between 6 to 12 min and the mixing temperature was set at 230°C. Sample $D_{reactor}$ was polymerized in a standard glass reactor under nitrogen atmosphere at 230°C.

Residual Monomer Characterization
Different methods have been proposed to determine the conversion of monomers to polymer. Among these methods, which include gravimetric technique

Table 1. Formulation of different polyamide samples polymerized in Haake mixer.

Code		Epsilon-caprolactam	Na-caprolactam	Hexamethylene diisocyanate
1	A	96	3	1
2	B	95	3	2
3	C	96	1	3
4	D	94	3	3
5	$D_{reactor}$	94	3	3
6	E	97	2	1
7	F	96	2	2
8	G	95	2	3
9	H	94	3	4
10	I	94	4	3
11	K	94	4	4

and GC-mass model Ailent 6890 series GC system 5793 Network MSD HP-5ms, we found that the gravimetric method was the most useful technique. This was based on the ratio of the mass of polymerized products of which the residual monomers were removed by solvent extraction. We used methanol as a solvent for Soxhlet extraction of unreacted ε-caprolactam for 24 h. Then, the samples were dried in a vacuum oven for 10 h. GC-mass was used for confirming the Soxhlet extraction results for the samples showing the lowest residual monomer content.

Weight-average Molecular Weight

The weight-average molecular weight, $\overline{M}_w$, of PA6 was determined by intrinsic viscosity measurements in 85% formic acid at concentrations of 0.1, 0.2 and 0.3 g/dL using a suspended level Ubbelohde viscometer thermostated at 27°C [10-12].

Physical and Mechanical Properties

After polymerization, all samples were dried in the vacuum oven for 24 h at 70°C. PA6 samples were shaped using compression moulding under nitrogen atmosphere in three steps. First the samples were pre-heated at 245°C for 15 min, then compressed at 30 MPa for 15 min and at the end they were cooled for 30 min.

The mechanical properties of the samples were evaluated at 23°C by tensile measurements using an Instron 6025 (England) machine according to the ASTM D 638 test method (10 mm/min). The impact properties of the samples were evaluated using a Zwick (5102 Germany) impact machine according to the ASTM D256 testing method. A minimum of five samples was tested in each series for determination of tensile and impact properties. The thermal properties were determined by differential scanning calorimetry (DSC) on Netzsch-Maia-200F3 instrument. Testing conditions were subjected to heat-cool-heat cycles from -50°C up to 240°C, where the heating and cooling rates were 10°C/min according to the ASTM D3418-03 test method.

For X-ray diffraction (XRD) a Siemens D5000 instrument was used and the samples were tested under 35 kV and 20 mA and detections were made between 15 and 30 degrees. All samples were disks of

1.6 mm in thickness and 25 mm in diameter.

Thermal gravimetry analysis (TGA) was performed for detecting degradation mechanisms of the samples. TGA tests were conducted under nitrogen flow from 35°C up to 600°C and then up to 1000°C in air. The heating rate was 10°C/min.

The morphology of polymers was observed by using scanning electron microscopy (SEM) model Hitachi S-4700 with cold field emission gun. All specimens were fractured in liquid nitrogen also for proving the existence of the fibril, the morphology of the thin cast film was used and then samples coated with Pt via vapour deposition to avoid charging by the electron beam.

In order to understand the chemical structure of the samples, infrared spectroscopy technique was used on thin films by using a Bruker, Equinox 55, FTIR spectrometer. The FTIR samples were moulded by compression at 250°C and 200 bars for 5 min. All the employed equipments are located at Iran Polymer and Petrochemical Institute.

RESULTS AND DISCUSSION

Synthesis of Polymer

Figure 1 shows the torque versus mixing time for different formulations. In all cases, the torque starts to increase at a time, which is called reaction or
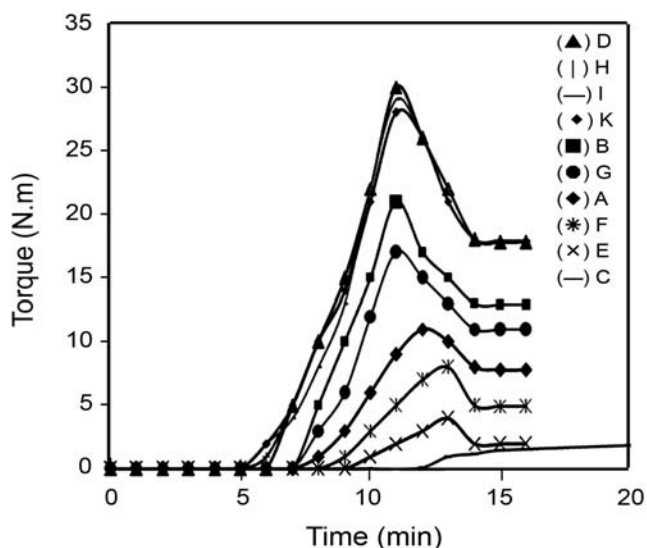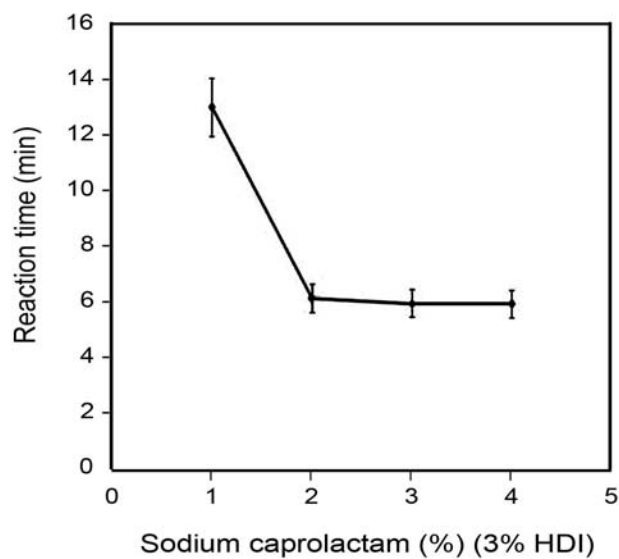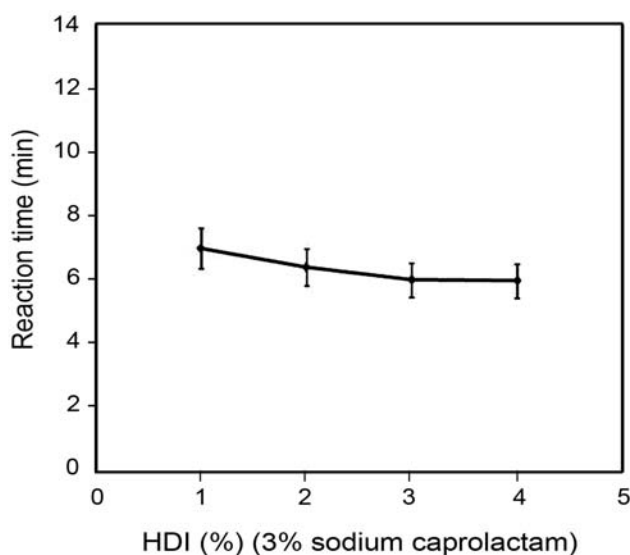

Figure 1. Torque-time curves at 150 rpm and 230°C for different formulations (Table 1) in a Haake mixer.

(a)

(b)

Figure 2. Effects of catalyst (a) and activator (b) on the initiation reaction time.

initiation time. Its duration has been between 6 min up to 12 min, depending on the formulation. It is known that the polymerization of caprolactam/Na caprolactam does not start without an activator. After the addition of only 1% of HDI, the polymerization takes place in a few minutes, which is due to the lower activation energy required for the nucleophilic attack of the anion caprolactam to its activated lactam group and the starting of the polymerization reaction by the presence of HDI. For all samples except sample C, the torque curves increased very rapidly

after about 5 min of mixing, indicating the starting point of the polymerization. It reached maximum 6 min later and then decreased very rapidly, indicating the end of polymerization [13].

Increasing the amount of catalyst (Na caprolactam) (Figure 2a) and the activator (HDI) (Figure 2b), it would decrease the time needed for the polymerization reaction, but the effect of Na caprolactam is more pronounced than that of HDI. The polymerization time of all samples in Haake mixer is less than 15 min, except for catalyst/activator:1/3 of formulation.

Since the molecular weight of PA6 is difficult to determine because of the limited solubility of PA6, two techniques were tried to characterize the molecular weight of PA6. First, the maximum torque during the polymerization of ε-caprolactam in the Haake mixer was used for comparing the molecular weight of different PA6 formulations. The maximum torque was attributed to the largest molecular weight of PA6 generated during the melt blending. It can be seen that increasing the amounts of catalyst and activator in the formulation increases the molecular weight of PA6 with a significant increase in torque as shown in Figure 1.

Characterization of Polymers

Intrinsic Viscosity Measurements
The molecular weight, $\overline{M}_w$, of PA6 was estimated from intrinsic viscosity measurements using [12]:

$$\overline{M}_w \approx \overline{M}_v = 2.81 \times 10^4 [\eta]^{1.35} \tag{1}$$

The results are reported in Table 2. It is seen that $\overline{M}_w$ decreases with decreasing catalyst and/or activator contents in the PA6 formulation. It has the same trend with the results determined by maximum torque in the Haake mixer. Both techniques confirm that the largest $\overline{M}_w$ is for the catalyst/activator:3/3 formulation (sample D). Moreover, a slight increase in $\overline{M}_w$ was observed for the same formulation prepared in the glass reactor (sample $D_{reactor}$). Also the $\overline{M}_w$ of PA6 of the catalyst/activator:3/3 formulation is larger than that of the PA6 commercial grade, which was determined using this technique [10-12].
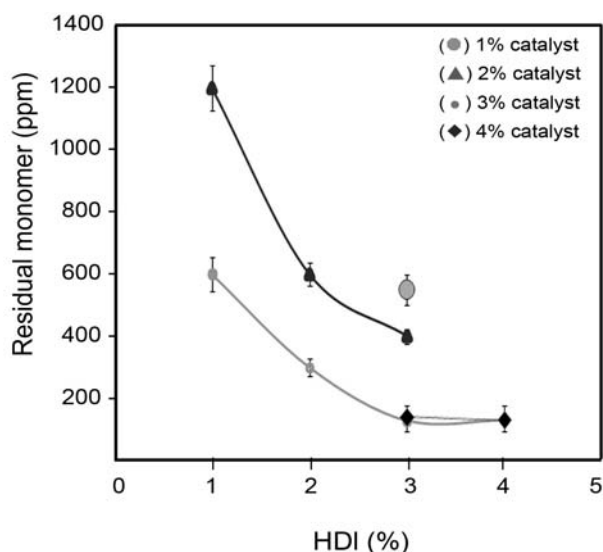
Residual Monomer Determination
The residual monomer was determined using two

Table 2. Intrinsic viscosity and molecular weight, $\overline{M}_W$ of PA6 samples and commercial PA6.

Code		$[\eta]$ (dL.g^{-1})	$M \times 10^{-4}$ (g/mol)
1	A	1.28	3.92
2	B	1.42	4.51
3	C	1.14	3.35
4	D	1.72	5.84
5	$D_{reactor}$	1.79	6.16
6	E	1.08	3.11
7	F	1.21	3.63
8	G	1.18	3.51
9	H	1.71	5.84
10	I	1.72	5.84
11	K	1.72	5.84
12	Commercial PA6	1.60	5.30

Figure 3. Effect of catalyst and activator contents on residual monomer determined from Soxhlet extraction.

techniques: solvent extraction and a GC-mass technique. However, the GC-mass technique was used only with the best PA6 formulation in order to confirm the solvent extraction result. Methanol was used as the extracting solvent for removing the unreacted caprolactam monomers. Figure 3 shows the effect of catalyst concentration on the residual monomer content of the samples against percentage activator content. This figure clearly shows that increasing the both contents dramatically affects the residual monomer content. The residual monomer content was reduced to 129 PPM for PA6 containing 3% catalyst and 3% activator. However, no more reduction was obtained when the sodium caprolactam and HDI were increased over 3%. The result obtained via the GC-mass test show that the residual monomer content in sample D containing 3% catalyst and 3% HDI was 129 ppm, confirming the validity of Soxhlet extraction results.

In the results reported by Liang et al., Ueda et al.,

and the other researchers [1,10,11], the maximum conversion of ε-caprolactam was reported to be around 98% (2% residual monomer). However, the residual monomer content (Figure 3) in this work was about 129 ppm; hence much lower than reported in the cited references for the same molecular weight. The improvement in the polymerization efficiency is believed to be caused by the use of a double functional cyanate (HDI).

Morphology
Figures 4a-4f show SEM morphologies of PA6 produced via anionic ring opening polymerization. These consist of two phases, the first one is the normal matrix and the second one is nanofibril. For the glass reactor based sample (Figures 4e and 4f) it is clearly shown that the size of the nanofibril is larger than samples produced in the Haake mixer (Figures 4a and 4b).

It is observed from Figure 5 that SEM results

Table 3. Characteristics of the nanofibrils.

Sample	Length (nm)	Diameter (nm)	Aspect ratio (L/D)	Concentration of nanofibrils (μm^2)
D	550	75	7.33	9
$D_{reactor}$	630	75	8.40	9
H	900	76	12.00	9

5 µm

1 µm

(a)

(b)
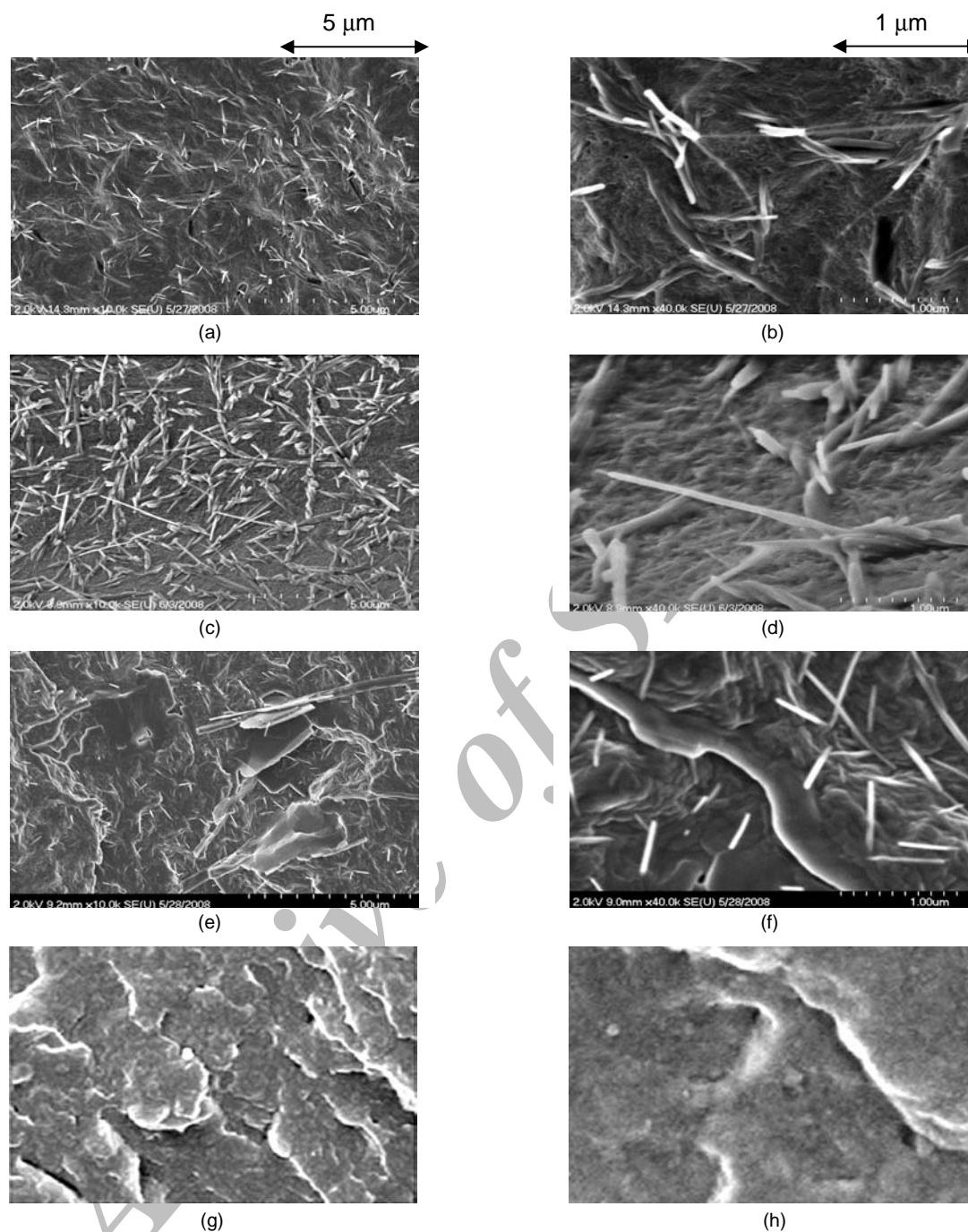
(c)

(d)

(e)

(f)

(g)

(h)

Figure 4. SEM micrographs for polyamide sample D (a and b), sample H (c and d), sample D$_{reactor}$ (e and f) and commercial PA6 (g and h).

which are taken from thin cast film also show similar nanofibril.

By increasing the level of HDI, the size of the nanofibril became larger as well, but the diameter and number of fibril remained almost the same, as shown in Table 3. The SEM micrographs of commercial PA6 (Figures 4g and 4h) do not show any fibrous morphology.

Because the HDI is an activator, increasing amount of activator can increase active polymerization sites. Due to this action, more value of catalyst must be involved in polymerization process. This effect can improve efficiency of polymerization and increase the size of nanofibrils. HDI has two active sites for polymerization and it is very sensitive against impurities such as humidity. Each site of the activator
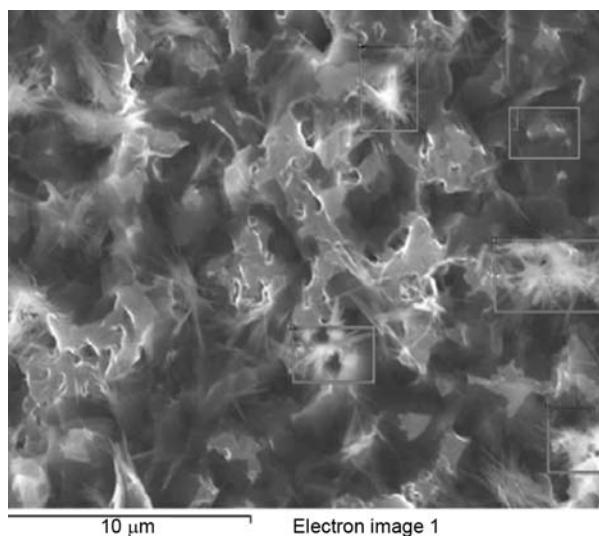
10 μm   Electron image 1

Figure 5. SEM micrograph of sample D as a cast thin film.

greatly influences the polymerization degree and the resultant chain length. Sudden inactivation of a site during polymerization terminates the growing polymer chains propagated from that site. However, polymerization will continue from the other active sites to produce higher molecular weight polymer chains with higher viscosity than those of immature chains. The difference between viscosities of two grades of PA6 is responsible for forming nanofibril composites during reactive melt blending. Finally, nanofibrils were produced during the reactive polymerization.

DSC Analysis

The DSC results reported in Table 4 are based on a melting endotherm peak during the heating scan and a single crystallization exotherm during the cooling stage. The crystallinity content of PA6 was estimated from ΔH_f measurements by the following equation [7,19]:

$$Crystallinity(\%) = \frac{\Delta H_{f\,sample}}{\Delta H_{f0}} \times 100, \ \Delta H_{f0} = 20$$

(2)

With increasing size of the fibril from samples H to D a shoulder appears near T_m, which can be assigned to the formation of nanofibril (Figure 6). Other researchers relate this melting point to the γ crystalline form [3,7].

DSC curves for samples D, $D_{reactor}$ and H show the occurrence of a shoulder as nanofibrils are formed and increased in length. Aliphatic polyamides, such as PA6, are well known for their strong hydrogen bonding (H-bonding) ability. Although all possible H-bonds are neutralized in the crystalline regions a vast majority are consummated in the amorphous regions [7]. Furthermore, a significant fraction of H-bonds remains even in the molten state. These strong H-bonding characteristics dominate the physical behaviour of PA6.

Table 4. DSC results for PA6 samples polymerized during melt blending and for the commercial PA6.

Code	T_c (°C)	T_{m1} (°C)	ΔH_c (J.g^{-1})	ΔH_{f1} (J.g^{-1})	χ_c (%)
A	155.2	205.0	15.9	18.7	9.12
B	156.0	205.4	16.8	19.2	9.36
C	156.5	203.5	15.1	16.5	8.04
D	157.4	214.2	48.1	51.2	24.95
$D_{reactor}$	168.6	216.6	54.7	55.2	26.91
E	154.2	203.0	15.2	17.3	8.44
F	155.0	207.0	14.6	17.8	8.70
G	152.0	208.0	15.6	18.0	8.80
H	158.0	212.0	46.3	47.2	23.02
I	157.2	212.0	45.3	45.2	22.04
k	157.4	213.0	44.2	45.6	22.24
Commercial PA6	173.2	219.0	65.3	64.8	31.60
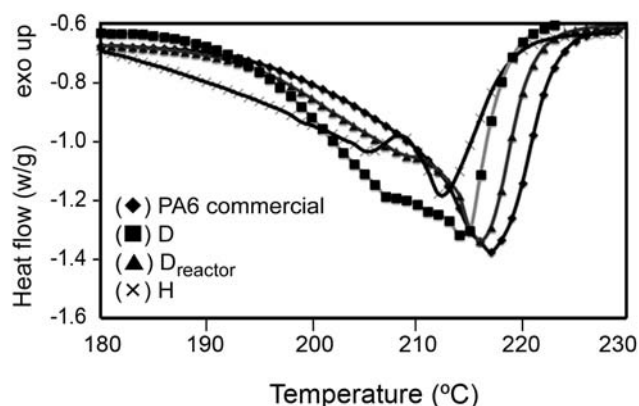
Figure 6. Melting DSC curves for the commercial PA6, D, D$_{reactor}$ and H samples.

Figure 7. Wide angle X-ray diffraction profile for sample D, sample D$_{reactor}$ and commercial PA6.

Comparing sample D$_{reactor}$ with that of sample D, their molecular weights were equal but sample D$_{reactor}$ had lower residual monomer content. The residual monomer increased the humidity absorption of PA6 and the humidity destroyed hydrogen bonds of the PA6 chains and reduced the crystalline content [13-15]. The higher T$_m$ for the high $\overline{M}_w$ may be the result of more ordered crystallites, e.g., fewer chain ends lead to a better chain folding and packing. This difference between the crystalline content affects T$_{m1}$ (melting point for the first cycle). The presence of impurity in the materials or the production of side products during melt blending in the Haake mixer is much more likely to happen than in a glass reactor under nitrogen atmosphere, so that impure products can reduce the molecular weight as observed in Table 2 for samples D and D$_{reactor}$. This reduction of molecular weight and increasing residual monomer content has lowered T$_c$ (crystallization temperature) due to the increasing molecular motion and plasticizing effect. Comparing samples D and H, the effect of molecular weight on T$_m$ is much more important than that on T$_c$. Increasing the level of catalyst and activator results in a PA6 of reduced residual monomer content, as mentioned in the case of caprolactam's effect on moisture absorption; as it also leads to an increased hydrogen bonding [3].

DSC thermograms show shoulders for T$_c$ and T$_{m1}$, which are assigned to the γ crystalline structure. The values reported in Table 3 for ΔH$_c$ (enthalpy of crystallization), ΔH$_{f1}$ (enthalpy of fusion for the first cycle), and %χ$_c$ (crystalline content) show the same trend.
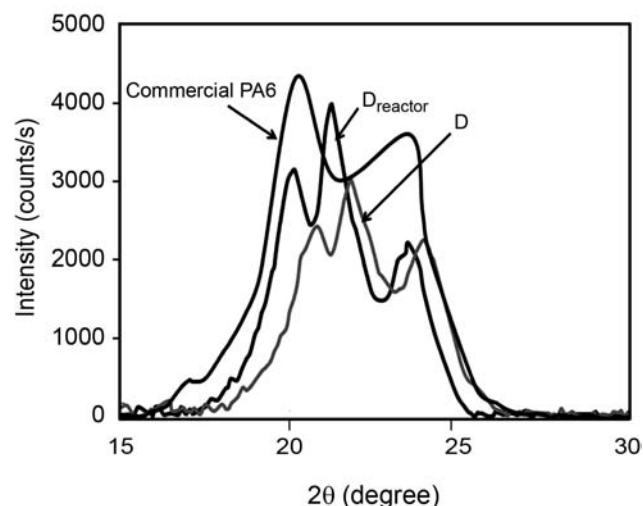
X-ray Analysis
Figure 7 shows the WAXD results for two PA6s prepared via anionic polymerization and compared to that of the commercial PA6. The WAXD pattern of the commercial PA6 (Figure 7) exists in α (α$_1$ and α$_2$) form, which is more thermally stable than the γ-form [3,16]. The polymerized PA6 samples of this work show three absorption peaks that are appeared in the α form (19.6° and 23.5°) and γ (21.3°). Samples produced in the glass reactor (D$_{reactor}$) show higher absorption peaks compared to samples prepared in a Haake mixer. For example, Hornsby et al. [3] obtained the α- and γ-crystalline forms by slowly cooling the samples in air, whereas, on annealing at 180°C for 90 min only the γ-crystalline form remained [3,7,17,18]. The sources of difference between the crystalline forms for the reactive polymerized PA6 and the commercial product are the narrower molecular weight distribution of the PA6 produced by anionic polymerization and the formation of less H-bonding, which leads to the creation of α- and γ-crystalline forms. The crystallinity content of PA6 was estimated from area (A) of each peak (Figure 8) using [19]:

$$\gamma \ (\%) = \frac{A_\gamma}{A\gamma + A_{\alpha 1} + A_{\alpha 2}} \times 100 \tag{3}$$

Table 5. XRD results for PA6 samples polymerized during melt blending and the commercial PA6.

Code	α_1 (%)	γ (%)	α_2 (%)	Crystalline content χ_c (%)
A	2.8	4.1	2.7	9.6
B	3.1	3.9	3.1	10.1
C	2.1	3.6	2.7	8.4
D	9.1	7.3	14.0	30.4
$D_{reactor}$	16.0	6.3	18.0	40.3
E	2.3	3.9	2.9	9.1
F	2.6	4.0	3.1	9.7
G	2.9	4.2	3.5	10.6
H	7.9	8.2	12.9	29.0
I	7.2	8.4	13.9	29.5
k	7.1	8.5	13.2	28.8
Commercial PA6	19.0	-	22.0	41.0

$$\alpha_1 \ (\%) = \frac{A_{\alpha 1}}{A_\gamma + A_{\alpha 1} + A_{\alpha 2}} \times 100 \qquad (4)$$

$$\alpha_2 \ (\%) = \frac{A_{\alpha 2}}{A_\gamma + A_{\alpha 1} + A_{\alpha 2}} \times 100 \qquad (5)$$

$$Crystallization \ (\%) = \frac{A_c}{A_c + A_a} \times 100 \qquad (6)$$

The XRD results reported in Table 5 confirm the crystalline contents calculated from the DSC results (Table 4). Table 5 shows that with the increasing γ-crystalline form, the size of the nanofibril increases (Figure 4 and Table 3) and shoulders in the melting peak DSC curves are more pronounced (Figure 5). Thus, it appears that the nanofibril improved formation of the γ-crystalline form.

TGA Analysis

Typical TGA showed the weight loss and derivative thermograms (DTG) of samples D, $D_{reactor}$, H, E and A were under nitrogen atmosphere but it changed to air atmosphere at 600°C. The degradation behaviour can be observed under both nitrogen and air environments in Figures 9a and 9b. The onset temperature of degradation (T_{onset}) and the temperature at maximum mass loss (T_{peak}) for the

first stage under nitrogen atmosphere up to 600°C are due to the fact that there are few residues of the coprolactam monomer in the matrix. This catalyst residue could induce the decomposition of PA6 at a lower temperature. Also a larger molecular weight can increase the thermal stability of PA6 samples. For a closer observation, the TGA data at 10, 30 and 50 wt% weight loss temperatures and T_{peak2} are summarized in Table 6.

It is found that for the larger molecular weight PA6 samples the thermal stability increases to higher temperatures, like 10.6°C for 10%, 26°C for 30% and
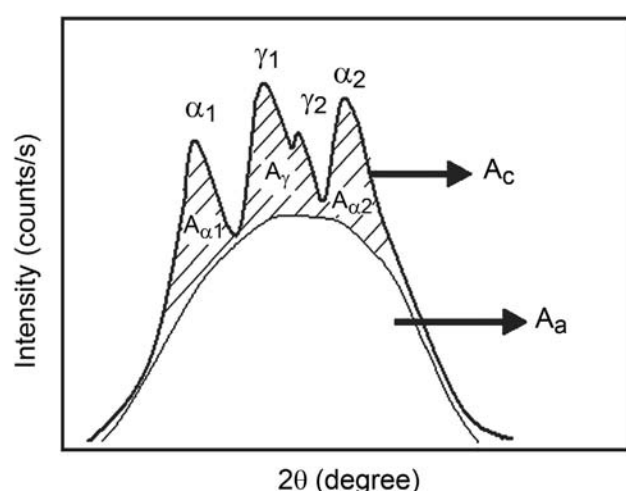

Figure 8. Schematic XRD wide angle X-ray diffraction profile for PA6 [19].

Table 6. TGA data for different formulations of melt polymerized PA6.

| Sample	$T_{10\ wt\%}$ (°C)	$T_{30\ wt\%}$ (°C)	$T_{50\ wt\%}$ (°C)	T_{peak2} (°C)
D	278.8	302.2	317.8	340.5
D$_{reactor}$	287.0	327.0	355.0	363.5
H	277.4	300.8	316.8	327.5
A	278.0	300.0	312.0	323.0
E	276.4	301.0	312.0	320.0

43°C for 50% weight loss. The differences between the curves for samples D, D$_{reactor}$, H, A and E in Figure 9b and data of Table 6 are due to differences in molecular weight (Table 2).

The differences between T_{peak2} for samples D and H, which have very similar molecular weights, may be caused by a difference in their molecular structures. Samples D and H have the same residual monomer and molecular weight, but sample H has more nanofibrils than sample D as shown in Figure 4 and Table 3. It appears that the presence of nanofibrils decreases T_{peak2}.

IR Analysis

FTIR absorptions of the PA6 samples made by reactive blending and the commercial PA6 are compared in Table 7. Close agreement is observed and the slight differences in the intensities and positions of the bands, especially the NH and CH$_2$ bands, are related to the polymer molecular weight.

The NH hydrogen absorption bands at 3270, 3301 and 3315 cm^{-1} for sample D$_{reactor}$ ($\overline{M}_w = 6.167$

(a)

(b)
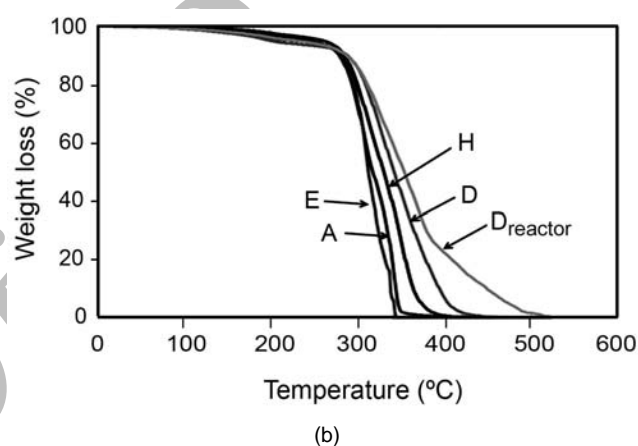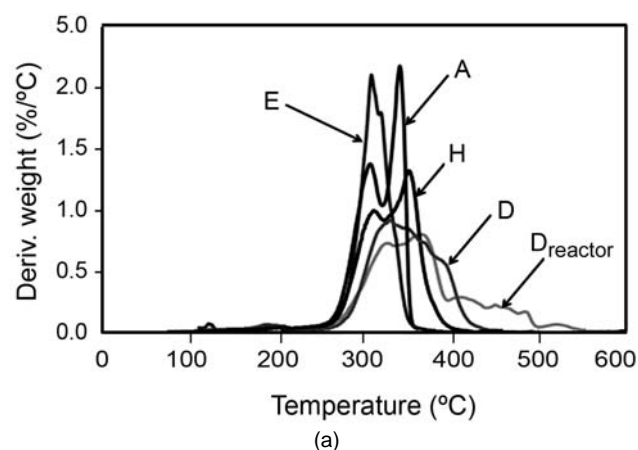
Figure 9. DTG (a) and TGA (b) curves for samples D, D$_{Reactor}$ and H.

$\times\ 10^4$ g/mol), the commercial PA6 ($\overline{M}_w = 5.30 \times 10^4$ g/mol), and sample A ($\overline{M}_w = 3.9313 \times 10^4$ g/mol), respectively, show an increase in the frequency of absorption with increasing molecular weight. The observed decrease in the position of these bands to

Table 7. Assignment of the FTIR absorption bands for the commercial PA6 and PA6 samples made by reactive blending.

Band assignment (cm^{-1})	A	B	C	D	D$_{reactor}$	E	F	G	H	I	K	Commercial PA6
NH Stretching H-bonded	3315	3310	3321	3290	3270	3322	3316	3320	3290	3290	3290	3301
CH$_2$ asymm. (aliphatic)	2910	2915	2910	2950	2980	2905	2950	2950	2950	2950	2950	2930
CH$_2$ symm. (aliphatic)	2860	2860	2855	2852	2850	2858	2860	2855	2852	2852	2852	2850
Amide I, C=O	1680	1670	1670	1666	1665	1681	1670	1677	1666	1666	1666	1650
Amide II, NH	1552	1550	1552	1545	1545	1552	1545	1550	1545	1545	1545	1550
-	1470	1473	1470	1475	-	1470	1475	1475	1475	1475	1475	1475
-	1461	1461	1461	1461	1461	1461	1461	1461	1461	1461	1461	1461
-	1440	1440	1440	1440	1445	1440	1440	1440	1440	1440	1440	1440
CH$_2$ deformation	1420	1420	1420	1420	-	1420	1420	1420	1420	1420	1420	1420

Table 8. Mechanical properties of the commercial PA6 and the anionic polymerized PA6.

Code	Tensile properties			Impact properties
	Elongation-at-break (%)	Stress-at-break (MPa)	Young's modulus (MPa)	Notched impact (kJ/m^2)
A	3.0 (0.72)	5.0 (1.90)	45 (7.61)	2.2 (0.60)
B	12 (2.50)	12 (1.02)	193 (11.05)	2.9 (0.68)
C	76 (5.00)	64 (2.32)	621 (9.08)	10.9 (1.30)
D	130 (8.32)	69 (2.11)	964 (10.36)	13.2 (1.10)
D$_{reactor}$	160 (9.12)	87 (3.02)	1210 (11.60)	11.2 (1.12)
E	30 (2.05)	24 (3.11)	143 (13.21)	1.3 (0.32)
F	32 (2.00)	43 (4.51)	230 (11.25)	2.3 (0.95)
G	60 (3.12)	49 (3.38)	258 (12.20)	2.4 (0.65)
H	128 (5.31)	66 (3.82)	760 (10.20)	12.5 (1.02)
I	125 (7.31)	67 (4.62)	768 (9.52)	12.2 (0.98)
K	128 (9.11)	71 (4.25)	765 (10.32)	12.7 (0.85)
Commercial PA6	50 (3.52)	74 (5.20)	1030 (8.65)	8.0 (1.02)

lower wavenumbers appears to follow the increase in molecular weight of PA6 and the resulting increase in interchain hydrogen bonding.

The CH$_2$ stretching bands appear at 2950, 2930 and 2910 cm^{-1} for sample D, the commercial PA6, and sample A, respectively, also show an increase in frequency of absorption peak with increased molecular weight. The PA6 sample of the largest molecular weight shows only two absorption peaks around 1461 and 1445 cm^{-1}. The report published by Hornsby et al. [3] showed also the same effect of molecular weight on the absorption peaks [3,20]. Consequently, the order in the molecular weight of the polyamide according to their absorption bands is:

D$_{reactor}$ > D, H, I, K > commercial PA6 > B, F > C > A, G, E

Therefore, the absorption band position substantiates the results for the molecular weight reported in Table 7.

Mechanical Properties
Key results for the mechanical properties are reported in Table 8. The numbers in parentheses are the standard deviations. The best properties are obtained for the formulation D which contains 3% sodium

caprolactam and 3% HDI, and increasing the level of catalyst and activator to more than 3% did not change the mechanical properties significantly. For samples D and D$_{reactor}$ the mechanical properties are close or even better than those of the commercial PA6. Anionic polymerization method can produce polymers with lower PDI (polydispersity index) than other polymerization methods which can improve impact properties. Also according to molecular weight detection of PA6 samples (Table 2) higher elongation-at-break of sample D$_{reactor}$ may be related to higher molecular weight of this sample.

CONCLUSION

In this work, a reactive polymerization of ε-caprolactam inside an internal Haake mixer has been realized. Using a wide range of characterization techniques such as XRD, GC-mass, DSC, TGA and tensile strength and impact the properties of the PA6 samples produced have been analyzed. The results showed that by adjusting the activator and the catalyst level the physical and mechanical properties of the anionic polymerized PA6 samples approached those of commercial grade produced via other methods. Other results of interest for this work are

the negligible residual monomer content and the high polymerization rate. Finally, nanofibrils were produced during the reactive polymerization.

REFERENCES

1. Zhang CL, Feng LF, Hu GH, Grafting of polyamide 6 by the anionic polymerization of ε-caprolactam from an isocyanate bearing polystyrene backbone, *J Appl Polym Sci*, **101**, 1972-1981, 2006.

2. Wu L, Jia Y, Sun S, Zhang G, Zhao G, An L, Numerical simulation of reactive extrusion processes of PA6, *J Appl Polym Sci*, **103**, 2331-2336, 2007.

3. Hornsby PR, Tung JF, Characterization of polyamide 6 made by reactive extrusion. II. Analysis of microstructure, *J Appl Polym Sci*, **54**, 899-907, 1994.

4. Yang M, Gao Y, He JP, Li M, Preparation of polyamide 6/silica nanocomposites from silica surface initiated ring-opening anionic polymer-ization, *Express Polym Lett*, **1**, 433- 442, 2007.

5. Suteu D, Bilba D, Dan F, Synthesis and character-ization of polyamide powders for sorption of reactive dyes from aqueous solutions, *J Appl Polym Sci*, **105**, 1833-1843, 2007.

6. Ji Y, Li W, Ma J, Liang B, A novel approach to the preparation of nanoblends of poly(2,6-dimethyl-1,4-phenylene oxide)/polyamide, *Macromol Rapid Commun*, **626**, 116-120, 2005.

7. Fornes TD, Paul DR, Crystallization behavior of nylon 6 nanocomposites, *Polymer*, **44**, 3945-3961, 2003.

8. Shields RJ, Bhattacharyya D, Fakirov S, Fibril polymer-polymer composites: morphology, properties and applications, *J Mater Sci*, **43**, 6758-6770, 2008.

9. Vallejo FJ, Eguiaza bal JI, Naza bal J, Compatibilization of PP/Vectra B "in situ" composites by means of an ionomer, *Polymer*, **41**, 6311-6321, 2000.

10. Ueda K, Yamada K, Nakai M, Matsuda T, Hosoda M, Tai K, Synthesis of high molecular weight nylon 6 by anionic polymerization of ε-caprolactam, *Polym J*, **28**, 446-451, 1996.

11. Ueda K, Nakai M, Hosoda M, Tai K, Stabilization of high molecular weight nylon 6 synthesized by anionic polymerization of ε-caprolactam, *Polym J*, **28**, 1084-1089, 1996.

12. Li Y, Yang G, Studies on molecular composites of polyamide 6/polyamide 66, *Macromol Rapid Commun*, **25**, 1714-1718, 2004.

13. Whelan T, *Polymer Technology Dictionary*, Chapman & Hall, 1994.

14. Kohan MI, *Nylon Plastics*, Wiley, Chichester, 1973.

15. Paramoda KP, Liu T, Effect of moisture on the dynamic mechanical relaxation of polyamide-6/clay nanocomposites, *J Polym Sci Part B*, **42**, 1823-1830, 2004.

16. Bureau MN, Denault J, Cole KC, Enright GD, The role of crystallinity and reinforcement in the mechanical behavior of polyamide-6/clay nanocomposites, *Polym Eng Sci*, **42**, 1897-1906, 2002.

17. Yeh JL, Kuo JF, Chen CY, Adiabatic anionic polymerization of caprolactam in the presence of *N*-acylated caprolactam macroactivator: kinetic study, *J Appl Polym Sci*, **50**, 1671-1681, 1993.

18. Havlice J, Brozek J, Sachova M, Novakova V, Roda J, Polymerization of lactams, non-activated anionic polymerization of ε-caprolactam initiated with the sodium salt of ε-caprolactam, *Macromol Chem Phys*, **200**, 1200-1207, 1999.

19. Aharoni SM, *n-Nylons, Their Synthesis, Structure, and Properties*, Wiley, 1997.

20. Davtyan S, Zakaryan H, Tonoyan A, Varderesyan G, On heat regimes of anion-activated polymer-ization of ε-caprolactam, *e-Polymer*, **073**, 1-8, 2007.